9. PROTECTION AGAINST BEAM LOSSES

The halo of the LHC beams must be absorbed by a collimation system before it hits the cold bore of the magnets. The probability of interception will be much larger than 400. This is achieved by an assembly of two-stage collimators and absorbers matched into a special insertion.

9.1 THE PURPOSE OF THE BEAM CLEANING SYSTEM

Beam growth and loss

In any high luminosity collider, the circulating beams are only stable within a small range of betatron amplitudes which we refer to as the "dynamic aperture". Beyond this aperture, they fall under the influence of nonlinear fields and diffuse outwards with ever increasing amplitude. Normally the beam lies well within this aperture but particles may be elastically scattered into this outer region and then diffuse slowly towards the vacuum chamber wall. The beam acquires a halo, a continuous flux of particles which will deposit most of their energy as a hadronic shower in the surrounding material. This will often be the superconductor of the magnets which, beyond a certain limit of energy deposition, will quench. With the high luminosity foreseen for the LHC the expected rate of deposition is much higher than the quench tolerance and we must provide a beam cleaning system which will intercept the particles before they reach the chamber wall. The probability of interception must be very high indeed and will require two or more stages of collimation.

Predicted loss rate

It was shown in chapter 4.2 that under normal operating conditions, when the sum of the luminosities over all interaction points in LHC is $L = 5\ 10^{34}\ cm^{-2}s^{-1}$, there will be a beam halo corresponding to a flux of

$$\frac{dN_0}{dt} = 4.10^9 \text{protons/s},$$

diffusing towards the vacuum chamber.

It is quite likely that all these protons hit the vacuum chamber at one azimuthal position where the beam, due to a combination of closed orbit misalignment and other errors, makes its closest approach to the wall. It is unpredictable where this will occur and whether they will hit the vertical sides or the horizontal surfaces of the chamber or, both together in different locations where beta happens to be large. The beam cleaning system must guard against the worst case in which the loss is in a single location.

Tolerable loss rate

It was shown in chapter 5.7 that the maximum tolerable rate of losses at any given point along the ring must not be larger than a critical value of

$$\frac{dN_c}{dt} = 10^7 \text{protons/s},$$

if the quenching of an superconducting magnet is to be avoided.

Required interception efficiency

Obviously, most of the halo must be absorbed in an area which is free of superconducting elements and, if the interception method has an efficiency, η, then the fraction of particles avoiding interception, must be less than

$$(1-\eta) = \frac{dN_c/dt}{dN_0/dt} = \frac{10^7}{4\times10^9} = \frac{1}{400}.$$

Since losses are expected to be high, the beam cleaning section must not contain radiation sensitive elements, and if there are any in adjacent regions they must not be too close unless they are efficiently protected.

9.2 FEATURES OF THE BEAM CLEANING SYSTEM

Beam sizes

We assume the distribution of beam amplitudes is gaussian $\sigma = (\varepsilon\beta)^{1/2}$ as the r.m.s. beam width (see chapter 2.1). Table 9.1 collects together the beam sizes at the 1σ and 6σ contours at various values of β around the ring. The primary collimators will be placed at approximately 6σ for the high energy beam. They will then be matched to the aperture of the vacuum chamber and yet have sufficient clearance to accommodate the various orbit deformations discussed in chapter 4.

Choice of aperture limit

In the SPPS collider, a 6σ contour was found to be the best position for the primary collimators and this principle will be applied to all sections of the machine where aperture is restricted. In the LHC a 6σ contour (see table 9.1), also ensure sufficient clearance from the next aperture limitation which will be at the β_{max} of the physics insertions and is defined at the 10σ contour.

The impact parameter

One of the major difficulties that must be overcome in the design of collimators to intercept the halo is that a large fraction of the 8 TeV halo particles will hit the front face of an obstacle with a very small impact parameter, b. This, measured away from the collimator edge, is only 1μm (see fig. 9.1a). Such a small value excludes the use of a septum of any kind to peel away the particles, because no field can grow from zero to a useful value over such a small distance. It might be possible to consider a superconducting device, but the heat deposited when used for beam cleaning rules this out. The only remaining solution is to use a collimator.

Collimators

The collimator we propose is a block of material which has a flat inner face parallel to the trajectories of the halo particles. It must be long enough to ensure a high probability of hadronic interaction. The efficiency of the collimator is limited by multiple Coulomb scattering which slightly deflects the trajectory of the protons entering the block. If the impact parameter is too small, the proton can escape from the inner face of the block before it interacts, and enter the beam pipe again to be lost a few turns later. This effect is important and we will show in section 9.5 that additional collimators are required to absorb this secondary flux.

Choice of material

Three factors must be taken into consideration in choosing the material for a collimator jaw.

- A short absorption length. This favours dense materials with a high atomic mass.
- A long radiation length to minimise Coulomb scattering. This favours materials with a small atomic charge.
- We must be able to polish the material and it must remain optically flat to less than 0.3 μm in view of the 1 μ impact parameter.

Length of collimators

The third of these factors limits the practical length L_p of the jaw to ≤ 300 mm. We see in table 9.2, which is for L_p = 300 mm, that this constraint dictates the use of a heavy material. Tungsten seems to be the best choice for both its high density and its ability to be polished [1], and in the remainder of this chapter we base our design on this choice.

Multiple Coulomb scattering

In evaluating the effect of multiple Coulomb scattering, it is enough to compute the average angular kick, $\langle\theta\rangle$, and the corresponding spatial displacement, $\langle\Delta Y\rangle$, received by a proton going through the first interaction length, L = 100 mm, of tungsten. Beyond that distance the initial flux has already gone down by a factor 1/e. These quantities are computed for p = 8 TeV using the formulae 1 (a) and (b).

Table 9.1

Betatron beam sizes [mm].

	Injection		Top Energy	
	1σ	6σ	1σ	6σ
Arcs				
β_{min} = 29.5 m	0.48	2.88	0.12	0.79
β_{max} = 169.5 m	1.15	6.91	0.28	1.67
Physics interactions (IR)				
β_{min} = 4/0.5 m	0.25	1.50	0.015	0.09
β_{max} = 260/4000 m	1.43	8.55	1.35	8.11
Other IR.				
β_{min} = 15 m	0.34	2.05	0.08	0.50
β_{max} = 250 m	1.40	8.39	0.34	2.03
β_{max} = 620 m	2.20	13.21	0.53	3.19

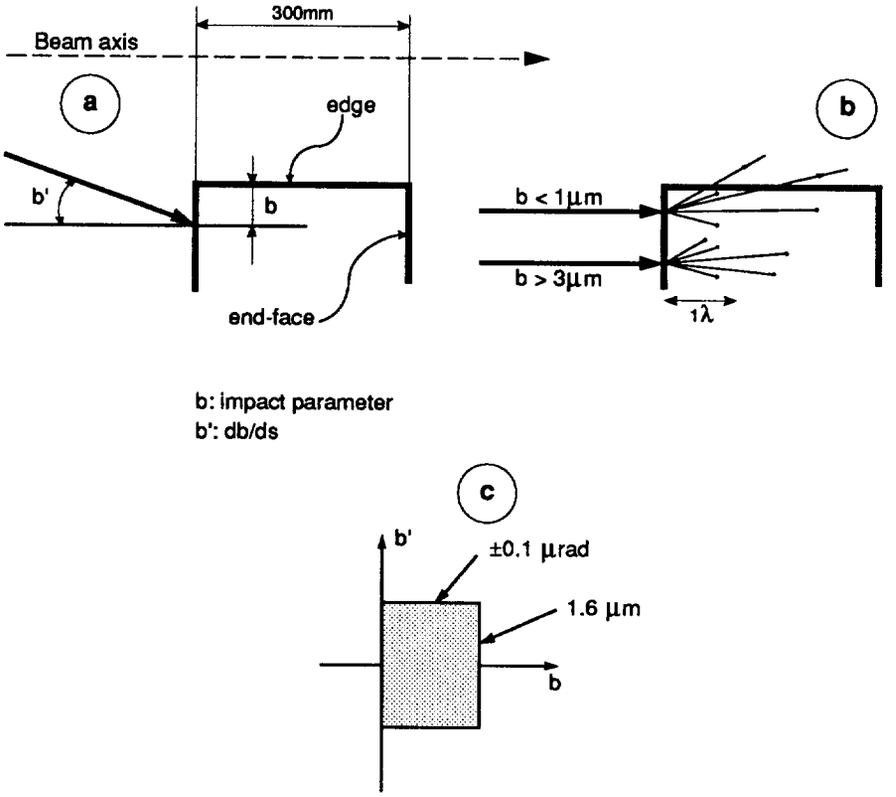

Figure 9.1: Collimators details.

a) A collimator jaw and some related definitions.
b) Efficiency limitations because of multiple Coulomb scattering.
c) Expected impact parameter distribution on LHC primary collimator.

Table 9.2

Parameters of possible collimator jaw materials [2].

	Be	Al	W
Nuclear interaction length λ_i [mm]	407	394	95.8
Radiation length L_R [mm]	353	89	3.5
$n_\lambda = Lp/\lambda_i$	0.74	0.76	3.1
e^{-n_λ}	0.48	0.47	0.045

$$<\theta>=\frac{14}{p[\mathrm{MeV}/c]}\sqrt{\frac{L}{L_P}}=10^{-5}\mathrm{rad.}, \qquad (1a)$$

and

$$<\Delta Y>=L\frac{1}{\sqrt{3}}<\theta>=0.6\mu\mathrm{m}. \qquad (1b)$$

We find that for an impact parameter, b ≤ 1 μm, a significant fraction of the protons escape from the inner face of the collimators. On the other hand if b > 3 μm, the probability of absorption is quite high (see fig. 9.1b).

The edge effect and inefficiency

Thus, the inefficiency of a collimator mostly stems from a small area of its inner face, approximately by <ΔY> deep. This quantity is proportional to 1/p and corresponds to what is usually called the edge effect. The inefficiency of one collimator, i.e. the ratio of the number of protons which do not make an inelastic interaction compared to the incoming flux, is given approximately by

$$(1-\eta)=\frac{<\Delta Y>}{\Delta b},$$

in which Δb is the width of the impact parameter distribution.

It will be shown in section 9.4 that a single collimator cannot absorb a sufficient fraction of the protons. Therefore, other collimators must be used to supplement its effect. The particles they must intercept include:

- Secondary particles created by inelastic collisions. Most of these have a momentum much smaller than the beam and will leave the acceptance rapidly, but a significant fraction might fall on the magnets at the entrance of the nearby arc. They must be absorbed before reaching the magnets. This is discussed in section 9.7.

- Primary protons which escape the primary collimator by multiple Coulomb scattering or after an elastic or diffractive inelastic collision. It will be shown in sections 9.5 and 9.6 that these can be absorbed efficiently by a well positioned secondary collimator.

9.3 THE IMPACT PARAMETERS OF THE HALO PARTICLES

Drift rate

The impact parameter of halo particles which diffuse in the transverse plane can be estimated if the average drift speed is known. The diffusion mechanism is related to non-linear phenomena such as beam-beam, magnetic imperfections, ripple of power supplies, etc., which may be coupled together through resonances. A quantitative prediction of the diffusion mechanism cannot be made with any degree of precision.

SPS measurements

The transverse drift speed was measured in the SP$\bar{P}$S collider [3] in an almost direct way. It was found that when the beam-beam constant, $\xi = 0.005$, is close to the foreseen value for LHC, the transverse drift speed (TDS) of the halo increases with the betatron amplitude and ranges from $v = 3\ \sigma/s$ at 5σ to $25\sigma/s$ at 8σ. We could assume that this is independent of beam energy but depends mainly on ξ. Then we may expect the TDS in the LHC, at the same distance measured in units of σ, will be at least as large as in the SPS. In fact it will probably be larger since the LHC will have larger magnetic imperfections and also because of long-range beam-beam effects which are absent in the SPS collider [4]. A higher drift speed might seem to offer a better efficiency due to a larger impact parameter but optical imperfections also induce larger beam losses. We adopt the conservative approach of assuming the drift speed does not scale with energy and couple this with a high estimate for the intensity of beam losses (see chapter 4.2).

Simulation tells us the impact parameter

We have obtained quantitative estimates of the impact parameter distribution by tracking protons around the LHC ring and by increasing the emittance at every turn according to the transverse drift speed. We shall come to the choice of β at the collimator in section 9.6, but we see from fig. 9.1c that for $\beta = 250$ m and at an amplitude of $y_o = 6\sigma$, the computed impact parameter distribution is approximately uniform in b and b' within the limits:

$$0 < b < 1.6\mu m \qquad \text{and} \qquad -1 < b' < +1\,\mu\text{rad}\,.$$

The average impact parameter doubles if y_o is increased by 1σ. (The quantities b and b' are defined in fig. 9.1c).

Unfortunately b is in the range where the edge effect will make the collimator inefficient. A significant flux will be re-emitted by the primary collimator so that a single collimator will not suffice.

9.4 SECONDARY FLUX FROM THE PRIMARY COLLIMATOR

We have taken the distribution of impact parameters b and b′ established above and used a Monte-Carlo program using the code ELSIM [1] to simulate the behaviour of protons incident on a tungsten collimator 400 mm long. The first results show that the effective length of the jaw is somewhat short, L = 250 mm. However this at least is shorter than the length that we can make sufficiently flat.

Jaw alignment is critical

The fraction of unabsorbed protons was computed as a function of the alignment angle b'_{jaw}. The result is shown in fig. 9.2. The inefficiency of a single collimator is still as high as 25% at the optimum alignment. We see that the alignment of the jaw must be adjusted on-line to a fraction of a micro-radian, since the flux leakage doubles at 5 μrad from that at the best angle. Also, the jaw or the beam must not oscillate by more than a fraction of a micron due to electrical ripple or mechanical vibrations. A prototype of such a device has been built and will be tested in the SPS collider.

Angular distribution for perfect alignment

The computed angular distribution of the outgoing protons which are close to the nominal beam momentum ($dp/p < 1\%$) is shown in fig. 9.3 for optimum alignment. The protons, which receive a positive kick, $b' > 0$, directing them further into the jaw,

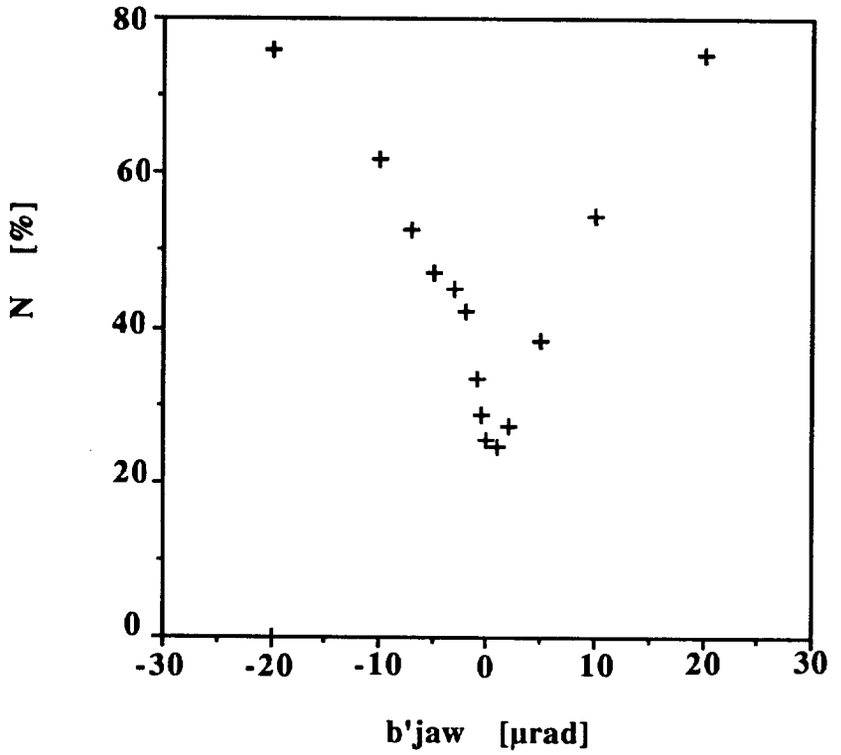

Figure 9.2: Integrated flux of 8 TeV protons leaking elastically out of the primary collimator, as a function of the misalignment angle of the jaw. The impact parameter distribution (b, b') is the one shown on fig. 9.1c.

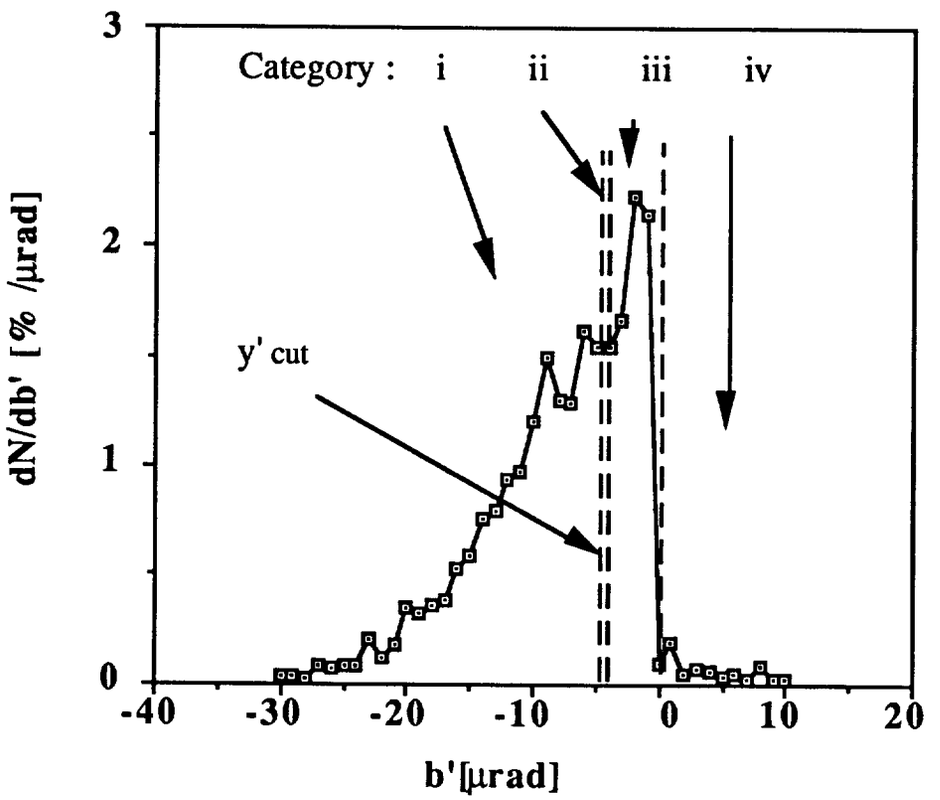

Figure 9.3: Angular distribution of 8 TeV protons leaking out the collimator, at the best angle of attack (see fig. 9.2). The cut of the distribution in four categories is discussed in section 9.7.

are well absorbed, while those on the negative side range between $-25 < y' < 0$ μrad, having an average kick of $y' = 7$ μrad. We shall discuss the means to catch these returning protons in the next section.

Effective edge thickness

We also computed the effective thickness of the inefficient edge zone of the collimator at 8 TeV by varying the impact parameter in the range $0 < b < 10$ μm but keeping $b' = 0$. At a finite misalignment, b', this quantity would obviously be larger. The relative secondary rate is given in fig. 9.4 and from this the effective thickness of the inefficient edge is computed as

$$d_\varepsilon = \int_0^\infty f(b)db = 0.7\mu m \ .$$

where f(b) is the relative leakage flux at a given impact parameter.

9.5 OPTICS OF A TWO-STAGE COLLIMATION SYSTEM

Second collimator to catch diverging particles

We consider a proton which escapes the first collimator with its inner jaw located at y_1 from the beam axis and assume it has the phase-space coordinates y_1 and y'_1.

The incoming proton is assumed to lie on a betatron ellipse which touches the collimator and therefore has $y'_1 = -(\alpha_1/\beta_1)y_1$. The divergence of the escaping proton is therefore the sum of the betatron divergence and b'_1, the deflection it receives in the jaw of C1 which follows the distribution shown in fig. 9.3 which we discussed in section 9.4. The protons escaping C1 are distributed in the transverse phase space (y, y') along a segment of a straight line. We show this for normalised phase-space in fig. 9.5. After a rotation of about $\Delta\psi = 150^o$, the segment of line corresponding to $y' < 0$ at C1 can be efficiently intercepted by a secondary collimator. For the less numerous protons which are re-emitted with $y' > 0$, a secondary collimator at small phase advance C1', is also necessary. The guiding principles for choosing the phase advance of these collimators are discussed in more detail in ref. [5].

Trajectory at second collimator

If C1 and C2 are located at s_1 and s_2 with the Twiss parameters (α_1, β_1) and (α_2, β_2) respectively and if the phase advance between C1 and C2 is $\Delta\psi$, then by using the transfer matrix $M = (m_{ij})$, the displacement of the re-emitted proton coordinate y_2 at C2 is

$$y_2 = m_{11}\, y_1 + m_{12}\left(y'_1 + b'_1\right).$$

The emission occurs at the phase space coordinate where the beam ellipse touches the vertical line corresponding to the collimator. For such a point one can write $y'_1 = -(\alpha_1/\beta_1)y_1$, then

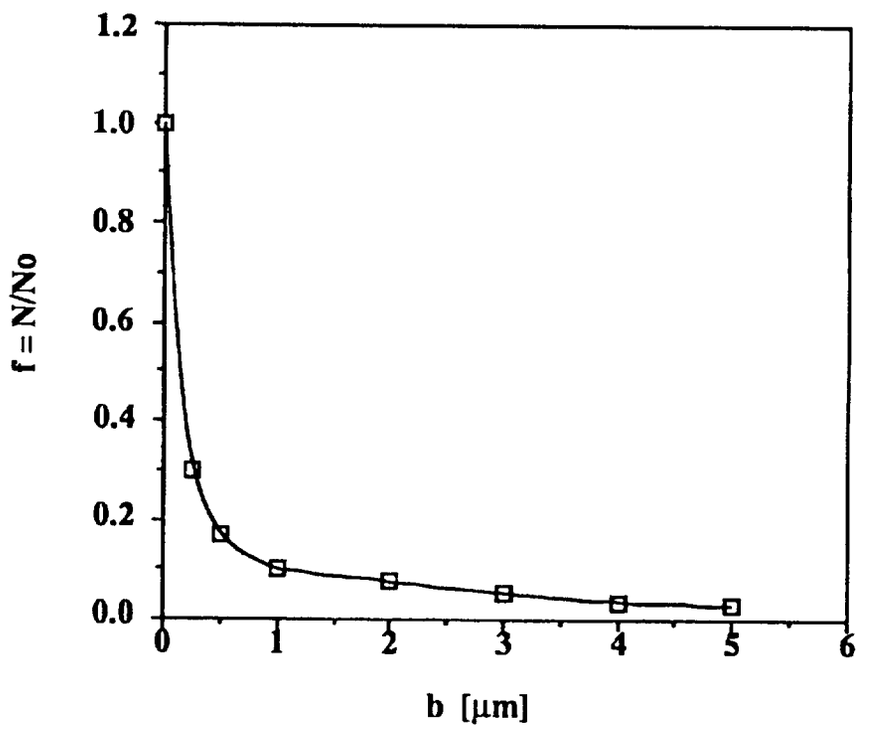

Figure 9.4: Relative flux leaking out of the collimator at 8 Tev as a function of the impact parameter b, while $b' = 0$.

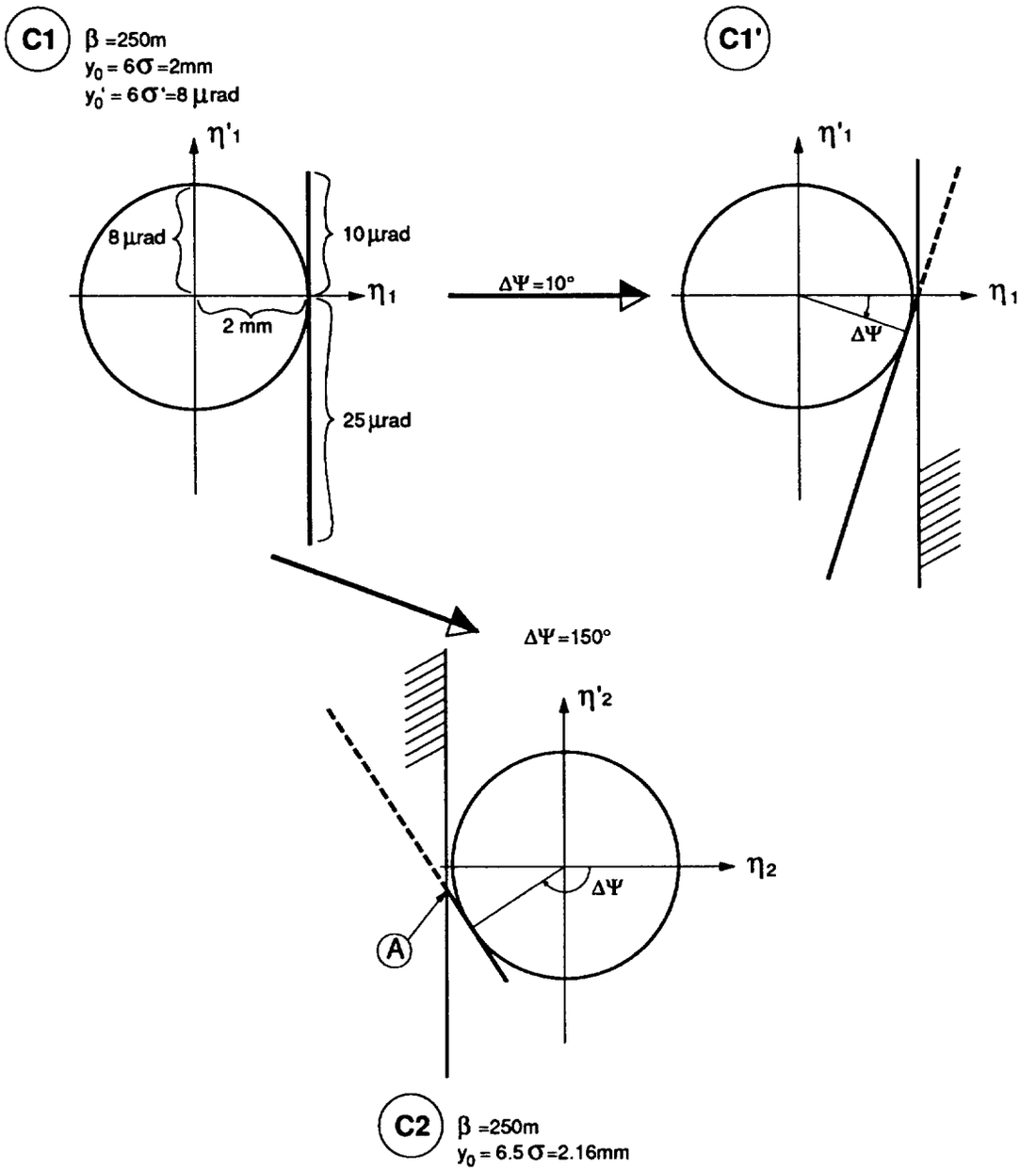

Figure 9.5: The normalised phase-space at the location of the collimators.

$$y_2 = \left(m_{11} - \frac{\alpha_1}{\beta_1} m_{12} \right) y_1 + m_{12}\, b'_1 \,.$$

Using the well known expressions for m_{11} and m_{12},

$$m_{11} = \sqrt{\frac{\beta_2}{\beta_1}} \left(\cos\Delta\psi + \alpha_1 \sin\Delta\psi \right), m_{12} = \sqrt{\beta_1 \beta_2} \sin\Delta\psi \,,$$

it appears that y_2 is independent of α_1:

$$y_2 = \sqrt{\frac{\beta_1}{\beta_2}}\, y_1 \cos\Delta\psi + \sqrt{\beta_1 \beta_2}\; b'_1 \sin\Delta\psi \,. \qquad (2)$$

We now consider y_2 at s_2 to be displaced by a small distance Δ away from the aperture defined by C1 at s_1 and we calculate the corresponding kick b'_1. The precise effect of this retraction, Δ, will be discussed later. Meanwhile we may write:

$$y_2 = -\sqrt{\frac{\beta_2}{\beta_1}}\, y1 - \Delta\ ,$$

the minus sign is introduced because C2 will actually be on the side opposite to C1 if the phase is roughly half a wavelength downstream. Then:

$$-\sqrt{\frac{\beta_2}{\beta_1}}\, y_1 - \Delta = \sqrt{\frac{\beta_2}{\beta_1}}\, y_1 \cos\Delta\psi + \sqrt{\beta_1\beta_2}\, b'_1 \sin\Delta\psi\ ,$$

which we then solve for b'_1:

$$b'_1 = -\frac{1}{\beta_1}\frac{1+\cos\Delta\psi}{\sin\Delta\psi} y_1 - \frac{\Delta}{\sqrt{(\beta_1\beta_2)}\sin\Delta\psi}\ . \qquad (3)$$

We see from equation 3 that a two-stage collimation system depends on four variables: b_1, b_2, $\Delta\psi$ and Δ.

We express y, and Δ in units of r.m.s. beam size:

$$y_1 = n\sigma_1 \quad \text{and} \quad \Delta = \delta_\sigma \sigma_2\ ,$$

and for convenience we substitute $\varphi = \pi - \Delta\psi$, then finally

$$b'_1 = -n\sqrt{\frac{\varepsilon}{\beta_1}} \cdot \left(\frac{1-\cos\varphi}{\sin\varphi} + \frac{\delta_\sigma}{n}\frac{1}{\sin\varphi} \right). \qquad (4)$$

This formula gives the cut-off made by C2 (at point A in fig. 9.5) from the angular distribution of the protons re-emitted at C1 (fig. 9.3) for given δ_n and φ. This angular cutoff, b′, expressed in units of normalised divergence, $(\beta_1/\varepsilon)^{1/2}$ is shown on fig. 9.6. It has a locus of minima which is approximately straight and which is given by

$$b'_1 = -\sqrt{\frac{\varepsilon}{\beta_1}} \cdot \varphi \quad \text{while} \quad \varphi(b'_1) = \sqrt{\frac{2\delta_n}{n}}\ .$$

Choice of δ_σ

Of course δ_σ must be small for efficient absorption of the halo. But there are practical limits to its lowest value set by mechanical vibrations, the drift of the stable orbit during a coast, and by power supply ripple, etc. We must ensure δ_σ is large enough that C2 never becomes the primary collimator in spite of these effects. We have chosen nominal values of $\Delta = 0.5\sigma$ and $\varphi = 0.5$ radians (a phase difference of $\Delta\psi = 150^o$). This is slightly beyond the minimum in b'_1, such that if we are forced to change δ_σ from 0.5 to 1.0, φ would then be optimum at that new position. This will minimise the sensitivity to the choice of δ_σ. The risk of being too close to the rapid increase of the function at the left of the minimum is also avoided.

Choice of beta values at the collimator

It still remains to select the best β values at C1 and C2. We see from equation 4 that the larger β_1, the smaller and the better will be the cutoff angle. Also, the impact parameter distribution at C1 will be magnified by a factor $\sqrt{\beta_1}$. A large β_1 thus increases the primary absorption, and it also increases the average y'_1 of the secondary flux which in turn produces large y_2 at C2.

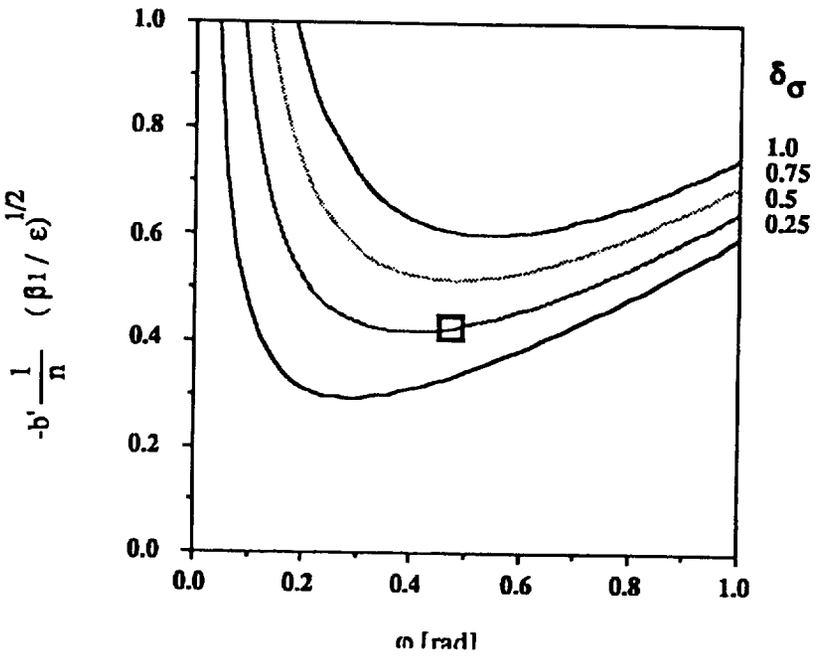

Figure 9.6: Cut-off in the angular distribution at C1 when C2 is set at a relative distance $\delta\sigma$ with n = 6. The square indicates the working point.

In figure 9.5 we see the particles scattered at C1 penetrate into C2 to an extent which is governed by the matrix element

$$m_{12} = (\beta_1 \beta_2)^{1/2} \sin \Delta\psi \, .$$

The term sin $\Delta\psi$ is fixed by other criteria, so Δy_2 will be maximised by choosing both β_1 and β_2 to have the largest possible value.

As the beam cleaning will be operational at any energy, the maximum β values should be compatible with the aperture limitations at injection energy. Furthermore no superconducting quadrupoles will be installed between C1 and C2 (see fig. 9.7). Then the largest reasonable β value at C1 and C2 will be $\beta_1 = \beta_2 = 250$ m.

Special insertion

The design of insertions for physics or for the dump cannot satisfy these constraints, summarised in the specification to be found in section 9.8. However, a special design of insertion which meets this specification has been found (see chapter 3.2.6). The numeric values for the transfer matrix elements used in the next section are computed from detailed lattice calculation and differ slightly from the nominal requirement defined above.

9.6 INEFFICIENCY OF THE TWO-STAGE COLLIMATION SYSTEM

No second chances

The net inefficiency of a two-stage collimation system is basically given by the flux, dN/dt, of protons which are leaking out of the whole C1-C2 system divided by the flux, $(dN/dt)_0$, incident on the primary collimator. In practice, this simple definition is difficult to apply since, in a circular machine, a proton leaking out of C2 may possibly be absorbed again by C1 after some turns and before it touches the vacuum pipe. To allow for this would require an almost perfect knowledge of the machine and we therefore assume that all protons which miss C2 end up on the vacuum chamber. This leads to an underestimate of the efficiency and is therefore somewhat conservative.

There are four categories of protons leaking out of C1. They are indicated on fig. 9.3 as different slices of the angular spectrum.

The two slices (i) and (iv) which contain 20% of the incoming flux, pass through the full length of the collimator and experience the full three interaction lengths of the collimator. The probability of not interacting is $5\ 10^{-2}$ and this is not small enough. We plan to install a back-up collimator or absorber after both C1 and C2 to further attenuate this flux with five interaction lengths of material. The back-up collimators are only 10° in phase after C1 and C2. The probability of survival is now only $3\ 10^{-4}$ and, when multiplied by the fraction of the angular spectrum in slices (i) and (iv), the leakage will be only $0.6\ 10^{-4}$.

Shallow impact in C2

In category (ii) are the protons which fall on the inefficient skin depth of C2. Their relative flux lies inside the angular domain $dy'_1 = d_e/m_{12} = 0.7/122 = 5.7\ 10^{-3}$ μrad. Here d_e is the effective thickness of the edge (section 9.4). There are $1.54\ 10^{-2}$ p/μrad in that region (see fig. 9.3), so that the probability of leaking in this way is $0.9\ 10^{-4}$.

No impact in C2

The protons which miss C2 are in category (iii), and their relative flux is $7.5\ 10^{-2}$. These protons have been tracked for a linear LHC, to which a Q spread of 0.02 was applied. If C2 is retracted by 0.5σ the protons fall again on C1 after 20 turns provided there are no aperture restrictions in between. Once the insertions around the experiments are decided we shall recalculate this effect to see if a local protection might be necessary. The impact parameter distribution on C1 is wide, b ~ 100 μm, but it is peaked at small b. We took all the flux below 10 μm which represents 40% of this category and applied conservative simplification by assuming b < 1 μm. This secondary input flux is added to the primary flux. It interacts with C1. We can then consider this 40% of the slice as a simple multiplying factor of $1 + 0.4 \cdot 7.5 \cdot 10^{-2} = 1.03$ applied to the halo.

Overall efficiency

The overall inefficiency is then

$$1 - \eta = 1.53\ 10^{-4} \, .$$

This inefficiency has been calculated for the standard set of parameters discussed in section 9.5, and assumes an impact parameters range $0 < b < 1\mu m$. This efficiency leaves some margin relative to the requirements expressed in section 9.1, but at this stage of the project important unknowns remains like the exact values of the impact parameters or of the halo intensity.

Required features of the insertion

We must reserve a dedicated area for the beam cleaning section with large β values, at the collimator locations. A phase advance of 150° between them is necessary to meet the absorption efficiency required by the high luminosity of LHC.

9.7 ABSORPTION OF INELASTICITY PRODUCED SECONDARIES

Recombination magnets deflect secondaries

It was shown in section 9.4 that 75% of the halo will interact inelastically in C1. The energy of the protons will be distributed among, on average, 25 particles, of average momentum $p = 4\%\ p_0$. These particles will be marginally absorbed in C1, some will interact again and produce tertiaries of even smaller momentum. We shall make use of the beam recombination magnets (see fig. 9.7) to discard and absorb all these secondaries. The first, D1-1, must then be positioned just behind C1, and the second, D1–2, in front of C2. Each of these will consist of six 5.3 m-long dipoles of SPS type, for a total bending power of 48 Tm. The kick to the 8 TeV beam will be 2.1 mrad. They will be warm dipoles which can accept a very high energy and radiation deposition.

Absorbers for secondaries

An absorber placed at the end of D1-1 will catch the particles of momentum $p < 0.68\ p_0$ if placed at the nominal vacuum chamber aperture (or more if set at a position deeper into the beam). Neutral secondaries will also be absorbed there, as indicated in fig. 9.7, and will require a vacuum chamber of special shape. Another absorber can be placed close to the central point if other equipment is to be installed at this location. Finally, an absorber will be placed at the entrance of D1-2, at ~12σ, for a momentum cut $p < 0.97\ p_0$. The second collimator C2, placed at 6.5σ, in addition to the absorption of elastic particles will achieve a cut, of $p < 0.992\ p_0$.

Fewer inelastic secondaries

The rate of inelastic secondaries of $p > 0.99\ p_0$ is much smaller than the rate of elastic and diffractive events generated in the simulation discussed in section 9.3. There is no need to correct the calculations of efficiency for this.

9.8 THE SPECIFICATION OF THE BEAM CLEANING INSERTION

One whole straight section must be dedicated to the beam cleaning system, in order to meet all the requirements stated in sections 9.5 and 9.7. The optics of the insertion should provide a drift space free of superconducting elements, approximately 100 m long. There will be collimators C1 and C2 at each end. The optics should also satisfy the following conditions:

1) The β at the collimators, $\beta_{C1} = \beta_{C2} = 250$ m (or more).

2) Between the collimators, a phase shift $\Delta\psi$ (C2–C1) = 150° This is only possible in a drift space if there is a waist in the middle of the insertion.

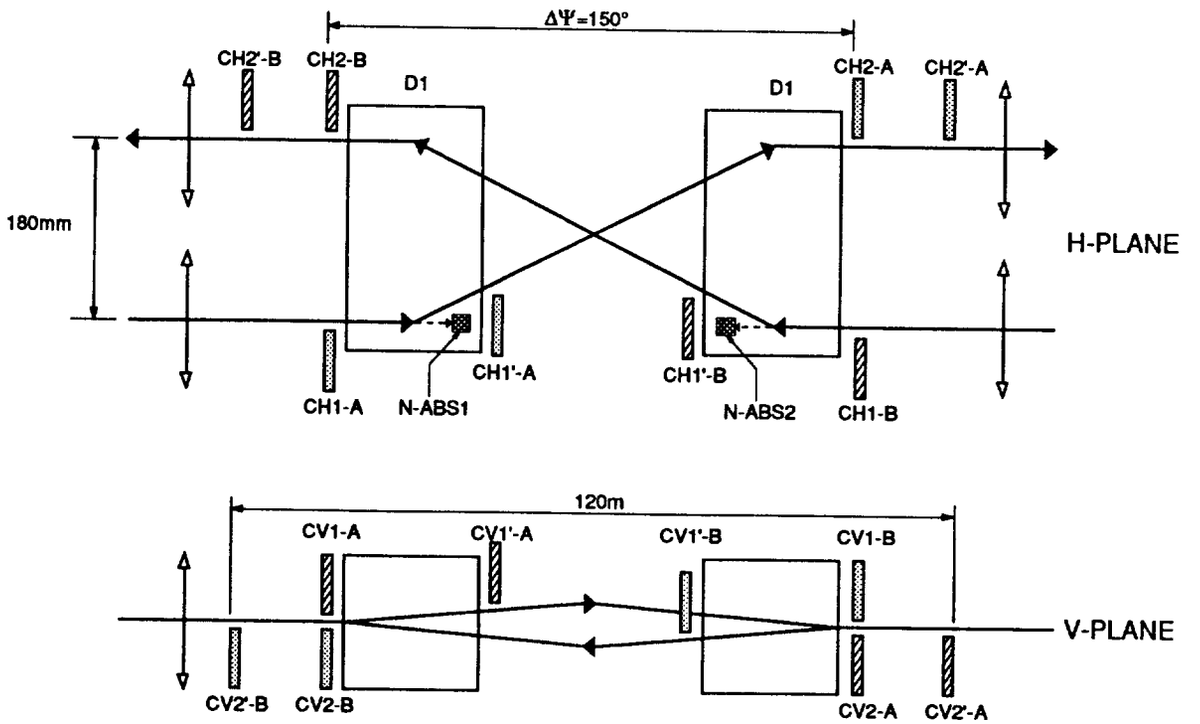

Figure 9.7: Schematic layout of the beam cleaning insertion. For clarity the proton absorbers are not shown. The phase advance is approximatively 150°. CH and CV are collimators. N-ABS are absorbers for neutral particles.

3) The whole system is simpler if the collimator positions are the same for both planes and if the system is symmetric for both beams around the centre of the straight section. Such an insertion has been designed.

4) The D1 magnets will be installed between C1 and C2, to sweep all the inelastic particles out of the acceptance. Some shielding will be installed inside the D1's and behind every collimator and absorber, to absorb the energy and the induced radiation.

The total power deposited by the halo of both beams will be of the order of

$$P_{tot} = 2(dN/dt)E = 2 \times 4\,10^{9}\,p/s \times 8\,TeV$$
$$= 6.4\,10^{22}\,eV/s = 10\,kW$$

The shielding necessary to prevent contamination of the whole section of the tunnel will occupy a great deal of space. The whole system is sketched in fig. 9.7.

* * *

References

[1] A. Van Ginneken, Phys. Rev. D37, 3292 (1988).

[2] The Particle Data Group, Review of Particle Properties, Phys. Lett. B, 204 (1988), p. 54.

[3] L. Burnod, G. Ferioli, J.B. Jeanneret, LHC note 117, Drift speed measurements of the halo in the SPS collider, CERN/SL/ Note 90-01, (EA), 1990.

[4] W. Herr, Tune shifts and spreads due to short and long range beam-beam interactions in the LHC, LHC Note 119, CERN/SL/90-06 (AP), (1990).

[5] J.B. Jeanneret, Phase difference between collimators in a collider, CERN/SL/EA/Note 90-01 (1990).